Title	N-channel thin-film transistors based on 1,4,5,8-naphthalene tetracarboxylic dianhydride with ultrathin polymer gate buffer layer
Author(s)	Tanida, Shinji; Noda, Kei; Kawabata, Hiroshi; Matsushige, Kazumi
Citation	Thin Solid Films (2009), 518(2): 571-574
Issue Date	2009-11
URL	http://hdl.handle.net/2433/87310
Right	c 2009 Elsevier B.V. All rights reserved.
Type	Journal Article
Textversion	author

N-channel thin-film transistors based on 1,4,5,8-naphthalene tetracarboxylic dianhydride with ultrathin polymer gate buffer layer

Shinji Tanida[a], Kei Noda[a,*], Hiroshi Kawabata[b], Kazumi Matsushige[a]

[a]*Department of Electronic Science and Engineering, Kyoto University, Katsura, Nishikyo, Kyoto 615-8510, Japan*

[b]*National Institute of Science and Technology Policy, Ministry of Education, Culture, Sports, Science and Technology, Kasumigaseki, Chiyoda, Tokyo 100-0013, Japan*

[*]Corresponding author. Tel.: +81 75 383 2307; fax: +81 75 383 2308

E-mail address: nodakei@kuee.kyoto-u.ac.jp (K. Noda)

(Abstract)

***N*-channel operation of thin-film transistors based on 1,4,5,8-naphthalene tetracarboxylic dianhydride (NTCDA) with a 9-nm-thick poly(methyl methacrylate) (PMMA) gate buffer layer was examined. The uniform coverage of the ultrathin PMMA layer on an SiO_2 gate insulator, verified by X-ray reflectivity measurement, caused the increase of electron field-effect mobility because of the suppression of electron traps existing on the SiO_2 surface. In addition, air stability for *n*-channel operation of the NTCDA transistor was also improved by the PMMA layer which possibly prevented the adsorption of ambient water molecules onto the SiO_2 surface.**

(Keywords) organic thin-film transistor, gate buffer layer, *n*-channel operation, electron traps, air stability

1. Introduction

N-channel conduction in organic thin-film transistors (OTFTs) has been researched actively for the purposes of realizing high-performance flexible complementary circuits (CMOS) with OTFTs and uncovering electron transport mechanisms in organic semiconductors [1]. In comparison with *p*-channel transistors based on pentacene, oligothiophene and so on, *n*-channel OTFTs show poorer characteristics. One of the main reasons for that is the air instability of many *n*-type organic semiconductors such as C_{60} [2] and perylene diimide derivatives [3,4] which are easily oxidized by ambient oxygen gases. Moreover, in the case of a silicon dioxide (SiO_2) gate insulator, silanol (SiOH) on SiO_2 surface can capture electrons in the *n*-channel region by generating anionic silicon monoxide (SiO^-) [5]. Actually, passivation of SiO_2 gate insulators with self-assembled monolayers (SAMs) [6] and polymer dielectrics [5,7,8] leads to the improvement of the electron transport properties in OTFTs. However, the details on reduction of electron traps with the surface passivation have not been sufficiently discussed yet.

In this study, we reported the improvements of electron mobility and air stability of *n*-channel OTFTs based on 1,4,5,8-naphthalene tetracarboxylic dianhydride (NTCDA) [9-11] by employing an ultrathin poly(methyl methacrylate) (PMMA) layer on an SiO_2 gate dielectric. The chemical structure of NTCDA is shown in Fig. 1(a). NTCDA is well known as an *n*-type organic semiconductor, but was reported to be unstable in air [9-11]. In previous studies, PMMA-coated gate dielectrics enabled *p*-channel TFTs to drive in ambipolar operation and displayed a potential of PMMA to reduce interfacial electron traps [7, 12]. In our work, we successfully fabricated a

9-nm-thick PMMA layer which covered an SiO_2 surface uniformly and showed a very smooth surface. Then, the increase of electron mobility and the air-stable operation of the NTCDA transistors were accomplished by utilizing this ultrathin PMMA gate buffer layer. From our results, the effects of this PMMA spacer on electrical characteristics of *n*-channel OTFTs were considered.

2. Experimental details

We investigated the effects of the ultrathin PMMA buffer layer on *n*-channel conduction in top-contact configuration of the NTCDA thin-film transistors with and without PMMA buffer layer (Fig. 1 (b) and (c)). These OTFTs were prepared as follows. PMMA and NTCDA were purchased from Aldrich. PMMA was purified with a precipitation method using a mixture of methanol and toluene in advance [13]. Using a PMMA/toluene solution, a PMMA layer was spin-coated onto a heavily doped *n*-type silicon wafer (< 0.02 Ωcm, size: 1.5 cm × 1.5 cm) which has a thermally grown SiO_2 with a nominal thickness of 100 nm, and baked for 15 min at 120°C with a hot plate. The thickness, the density and the surface/interface roughness of the PMMA and SiO_2 layer were determined in detail by X-ray reflectivity (XR) measurement system (ATX-G, Rigaku) in a specular ($\theta/2\theta$) configuration using Cu K_α radiation. The XR profile was analyzed with a Rigaku GXRR data-fitting software based on the theory of Parratt [14].

Next, once-sublimed NTCDA was thermally evaporated onto a bare SiO_2 and an SiO_2 coated with PMMA simultaneously at room temperature under the pressure of 1.0×10^{-4} Pa. The thickness of NTCDA films was 50 nm. Finally, 25-nm-thick gold was deposited onto NTCDA films

through a shadow mask to form source-drain electrode. The channel length and width were 50 μm and 1 mm, respectively.

The observation of the surface morphology of the NTCDA films was performed with an atomic force microscope (AFM) (JSPM-5200, JEOL) and the crystal structure was examined using an X-ray diffractometer (XRD) (MXP^3, BrukerAXS) with Cu K_α X-ray source. Electrical measurements of OTFTs were conducted in a vacuum (1.0×10^{-1} Pa), followed by the measurement in air, with a KEITHLEY 4200-SCS semiconductor parameter analyzer. The field-effect mobility for electron (μ_e) and threshold voltage (V_T) were obtained from transfer characteristics (drain-source current (I_D) vs. gate voltage (V_G)) in the saturation regime according to the following equation; $I_D = WC_i\mu_e(V_G - V_T)^2/(2L)$, where C_i is the gate capacitance. Here C_i was determined by an LCR meter (HP4263A, Agilent), by using a stacking structure of PMMA, SiO_2 and a heavily-doped Si substrate, on which upper Au electrodes were deposited by vacuum evaporation.

3. Results and discussion

3.1 Characterization of the PMMA layer

Figure 2 shows the result of XR measurement for the stacking structure of PMMA, SiO_2 layers and a Si substrate. An interference fringe arising from the PMMA layer was observed clearly. Fitting curve was fully coincident with the experimental result and showed that the PMMA film had the thickness of 9.2 nm, the density of 1.19 g/cm^3, and the surface roughness of 0.37 nm, respectively. And the thickness of the SiO_2 layer was estimated to be 107.2 nm at the same time.

From this result, it was concluded that the PMMA was spin-coated uniformly over the whole surface of SiO_2, because the surface roughness was very small and the density was the same as that of bulk PMMA (1.19 g/cm^3).

The capacitance of the SiO_2 film and a double layer thin film of PMMA and SiO_2 were measured to be 30.7 nF/cm^2 and 27.8 nF/cm^2, respectively, at a frequency of 100 Hz. From these C_i values and the thickness of each layer obtained by XR measurement, the dielectric constant was calculated to be 3.7 for SiO_2, and 3.1 for PMMA.

3.2 Structures of the NTCDA thin films

Figure 3 shows AFM images and XRD profiles of the NTCDA thin films. The surface morphology of semiconductor films on SiO_2 and PMMA was quite identical and we can see many small granular grains for individual specimens as seen in Fig. 3 (a) and (b). Moreover, XRD profiles of these two NTCDA films reveal almost the same diffraction intensity. For the NTCDA film on bare SiO_2, the peak position and the full width at half maximum (FWHM) in Fig. 3(c) were 2θ=11.74° and 0.18° for the first diffraction peak, 2θ=23.61° and 0.22° for the second one, respectively. For the specimen with the PMMA spacer (Fig. 3(d)), we obtained the peak position of 2θ=11.72° and the FWHM of 0.18° for the first peak, 2θ=23.60° and 0.24° for the second peak. From these similar XRD patterns, we can say that there was almost no difference in film structure of NTCDA on the bare SiO_2 and the PMMA layer, under the preparation condition employed in this study.

3.3 N-channel operation of the NTCDA TFTs in a vacuum

Transfer characteristics of the NTCDA TFTs with and without the PMMA layer in a vacuum are presented in Fig. 4. These two devices display clear *n*-channel operation. TFTs without PMMA layer showed the electron field-effect mobility of 3.6×10^{-4} $cm^2/(Vs)$ and the threshold voltage of -3.1 V. (In a previous report, NTCDA TFTs prepared on SiO_2 at room temperature revealed the electron mobility of 1.4×10^{-5} $cm^2/(Vs)$ in a vacuum [10].) On the contrary, we obtained μ_e of 1.0×10^{-3} $cm^2/(Vs)$ and V_T of -1.6 V from the TFT with the PMMA buffer layer. Thus, the electron field-effect mobility increased about three times by the PMMA spacer. Since there was no change in NTCDA thin film structure such as grain size and crystal structure as shown in Fig. 3, we could conclude that this improvement of the electron mobility was an effect of the PMMA spacer. However, the influence of dielectric properties of PMMA on the increase of the electron mobility can be negligible since the capacitance of the PMMA /SiO_2 double layer was smaller than that of the SiO_2 film.

Carrier transport in organic semiconductor films is governed by the hopping between localized states [15]. According to the theory of hopping transport, the field-effect mobility is inversely exponentially proportional to the barrier height for each hopping. It is possible that hydroxyls on SiO_2 gate insulators act as electron traps between hopping sites and increase the barrier height, resulting in the decrease of μ_e. The effect of interfacial electron traps can be suppressed by covering the SiO_2 surface with the PMMA layer. Namely, it might be suggested that

the ultrathin PMMA spacer could reduce the barrier height and increase the electron mobility as observed in our experiment. The suppression of the electron traps with the PMMA layer was also confirmed by the reduction of hysteresis phenomena for gate-biasing as shown in Fig. 4, indicating the decrease of electric charges trapped at the semiconductor/insulator interface.

3.4 N-channel operation of the NTCDA TFTs in air

Electrical characteristics of TFTs were evaluated in air. The measurements were performed three minutes after the exposure to air. The ambient humidity and temperature were 30% and 20 °C, respectively. No *n*-channel operation was observed for the TFT without the PMMA spacer as shown in Fig. 5 (a). Only transistor with the PMMA layer could show *n*-channel operation with μ_e of 1.3 × 10^{-4} $cm^2/(Vs)$ and V_T of 16.3 V, as presented in Fig. 5 (b). Therefore, ultrathin PMMA spacer could also improve the air stability of the NTCDA TFTs, although the gradual decrease of μ_e and the increase of V_T were observed after further exposure of the device to air. Finally, *n*-channel operation completely disappeared after the ambient exposure for a few hours.

NTCDA is mainly oxidized by oxygen under ambient condition. However, it is possible that the oxidation reaction of organic semiconductors is enhanced by the existence of moisture [16]. In ambient air, water molecules penetrate into NTCDA thin film and reach semiconductor/gate-insulator interface. In the case of using SiO_2 as gate insulator, water molecules are easily adsorbed onto the surface of SiO_2, because hydroxyls exist on the SiO_2 in the form of SiOH. Therefore, the oxidation of NTCDA proceeds rapidly in the *n*-channel region, resulting in the

degradation of electron transport properties. Besides, the generation of SiO^- caused by deprotonation of SiOH with H_2O can be also considered [17]. Negative charges of SiO^- presenting at the interface might cause a positive shift of the threshold voltage, which also leads to the deterioration of *n*-channel operation.

It can be expected that water molecules also become adsorbed onto the PMMA surface, because hydrogen bonding can be formed between water molecules and carbonyl oxygen of PMMA. However, the deprotonation of SiOH will not occur because H_2O molecules can not approach SiO_2 surface which is covered with PMMA. Therefore, the degradation of *n*-channel conduction in NTCDA films can be retarded. It can be said that the blocking effect of the PMMA layer against water adsorption onto the SiO_2 surface contributes to the air-stable operation of *n*-channel TFTs.

We would like to note that the 9-nm-thick PMMA film worked well as gate buffer layer, because it is normally quite difficult to control the thickness of insulating polymer films in a nanometer scale with keeping an uniform coverage over large areas. In this study, the excellent *n*-channel operation of the NTCDA transistor was demonstrated obviously. This fact reflects the sufficient coverage and small surface roughness of the prepared PMMA layer, which are supported by the results of the XR measurement.

4. Conclusions

The improvements of electron field-effect mobility and air stability of *n*-channel NTCDA

thin-film transistors were achieved by employing the ultrathin PMMA gate buffer layer. The 9-nm-thick PMMA film with a very small surface roughness was deposited uniformly onto the SiO_2 surface. This PMMA layer gave rise to three times increase in the electron mobility. Only transistors with the PMMA layer showed the *n*-channel operation in air. A series of experimental results suggest that even 9-nm-thick PMMA layer could passivate the SiO_2 surface, such that electron traps were decreased and the adsorption of ambient water molecules directly onto the SiO_2 film was suppressed.

Acknowledgments

This work was partly supported by Global Center of Excellence (G-COE) program of the Ministry of Education, Culture, Sports, Science and Technology of Japan.

(References)

[1] J. Zaumseil, H. Sirringhaus, Chem. Rev. 107 (2007) 1296.

[2] R. C. Haddon, A. S. Perel, R. C. Morris, T. T. M. Palstra, A. F. Hebard, R. M. Fleming, Appl. Phys. Lett. 67 (1995) 121.

[3] R. J. Chesterfield, J. C. Mckeen, C. R. Newman, P. C. Ewbank, D.A. da Silva Filho, J.-L. Brédas, L. L. Miller, K. R. Mann, C. D. Frisbie, J. Phys. Chem. B 108 (2004) 19281.

[4] S. Tatemichi, M. Ichikawa, T. Koyama, Y. Taniguchi, Appl. Phys. Lett. 89 (2006) 112108.

[5] L.-L. Chua, J. Zaumseil, J.-F. Chang, E. C.-W. Ou, P. K.-H. Ho, H. Sirringhaus, R.H. Friend, Nature 434 (2005) 194.

[6] D. Kumaki, S. Ando, S. Shimono, Y. Yamashita, T. Umeda, S. Tokito, Appl. Phys. Lett. 90 (2007) 053506.

[7] T. Takahashi, T. Takenobu, J. Takeya, Y. Iwasa, Appl. Phys. Lett. 88 (2006) 033505.

[8] J. Jang, J. W. Kim, N. Park, J.-J. Kim, Organic Electronics 9 (2008) 481.

[9] J. G. Laquindanum, H. E. Katz, A. Dodabalapur, A. J. Lovinger, J. Am. Chem. Soc. 118 (1996) 11331.

[10] K. Nakayama, M. Umehara, M. Yokoyama, Jpn. J. Appl. Phys. 45 (2006) 974.

[11] L. Torsi, A. Dodabalapur, L. Sabbatini, P. G. Zambonin, Sens. Actuators, B Chem. 67 (2000) 312.

[12] T. Sakanoue, M. Yahiro, C. Adachi, K. Takimiya, A. Toshimitsu, J. Appl. Phys. 103 (2008) 094509.

[13] N. Ohta, M. Koizumi, Y. Nishimura, I. Yamazaki, Y. Tanimoto, Y. Hatano, M. Yamamoto, H. Kono, J. Phys. Chem. 100 (1996) 19295.

[14] L. G. Parratt, Phys. Rev. 95 (1954) 359.

[15] M. C. J. M. Vissenberg, M. Matters, Phys. Rev. B 57 (1998) 12964.

[16] D. M. de Leeuw, M. M. J. Simenon, A. R. Brown, R. E. F. Einerhand, Synth. Met. 87 (1997) 53.

[17] D. Kumaki, T. Umeda, S. Tokito, Appl. Phys. Lett. 92 (2008) 093309.

(Figure captions)

Fig. 1. (a) Chemical structure of 1,4,5,8-naphthalene tetracarboxylic dianhydride (NTCDA) and device structures of a NTCDA TFT (b) without and (c) with a PMMA buffer layer.

Fig. 2. X-ray reflectivity profile for the PMMA film prepared onto a SiO_2/Si substrate. The solid line is the curve best-fitted for the experimental result (closed circle).

Fig. 3. AFM images of NTCDA thin films prepared on (a) a bare SiO_2 and (b) a PMMA layer are presented (scanning area: 3 μm × 3 μm). XRD profiles of the NTCDA film on (c) the SiO_2 and (d) the PMMA layer are also shown.

Fig. 4. Transfer characteristics of the NTCDA TFTs (a) without and (b) with the PMMA layer in a vacuum. The drain-source (V_D) voltage was set to be 60 V.

Fig. 5. Transfer characteristics of the NTCDA TFTs (a) without and (b) with the PMMA layer in air. The drain-source (V_D) voltage was set to be 60 V.

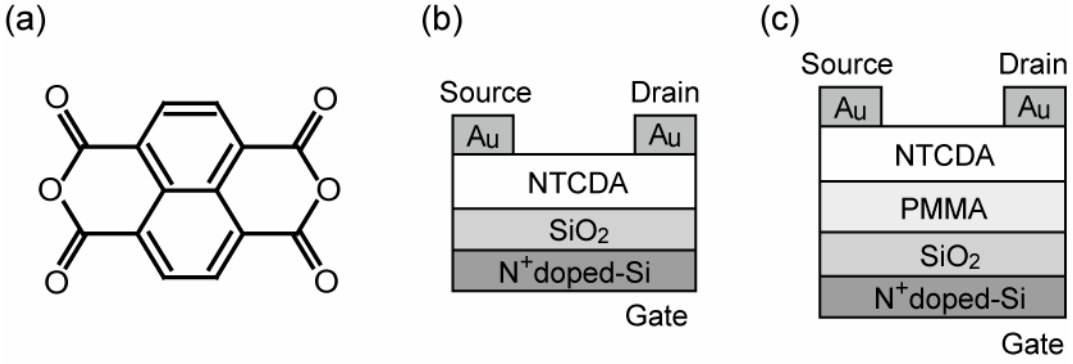

Fig. 1
S. Tanida et al.
(100%)

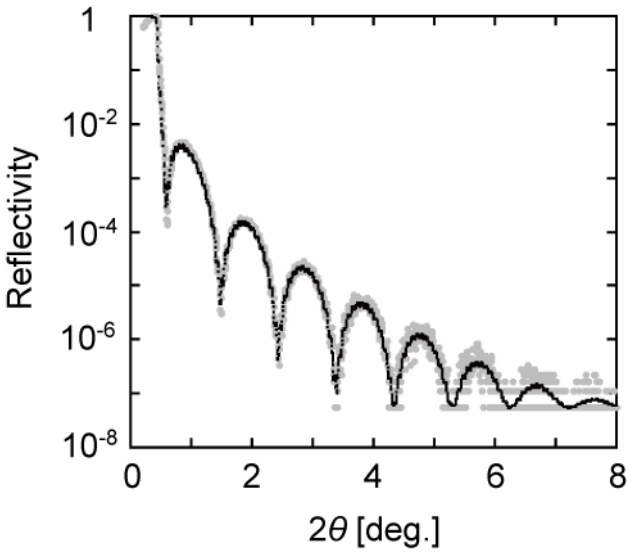

Fig. 2
S. Tanida et al.
(100%)

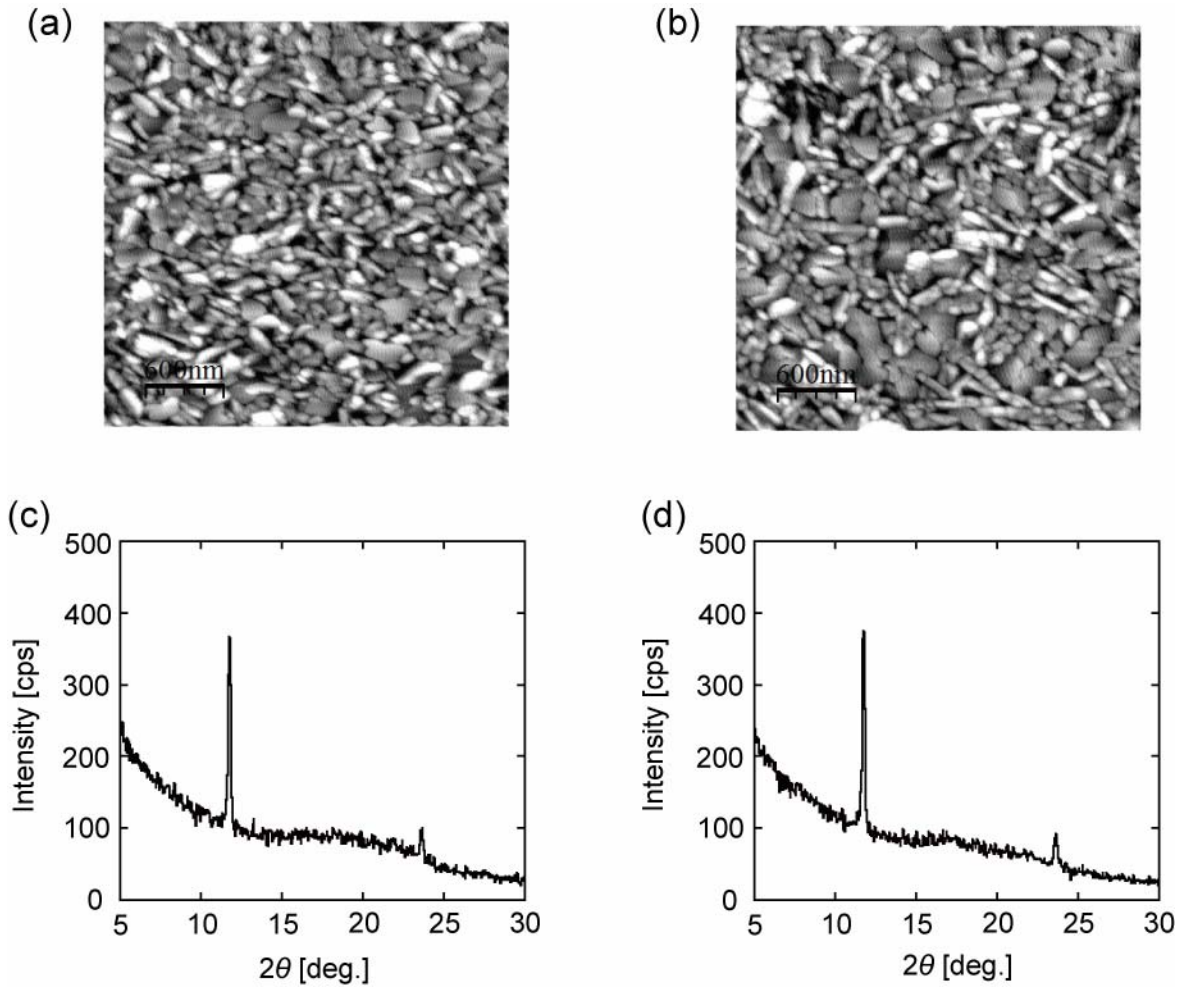

Fig. 3
S. Tanida et al.
(100%)

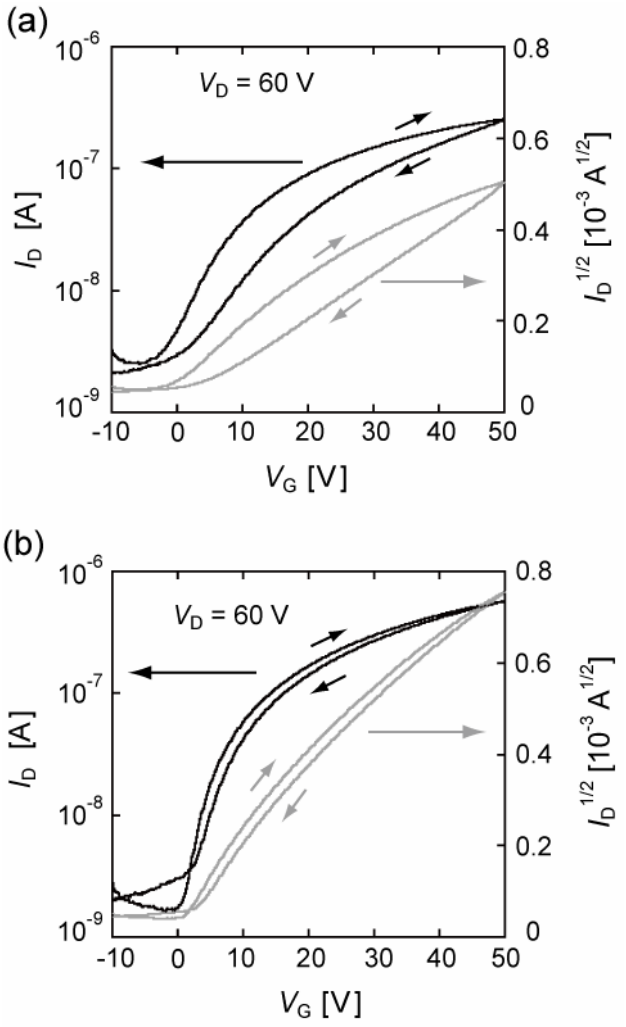

Fig. 4
S. Tanida et al.
(100%)

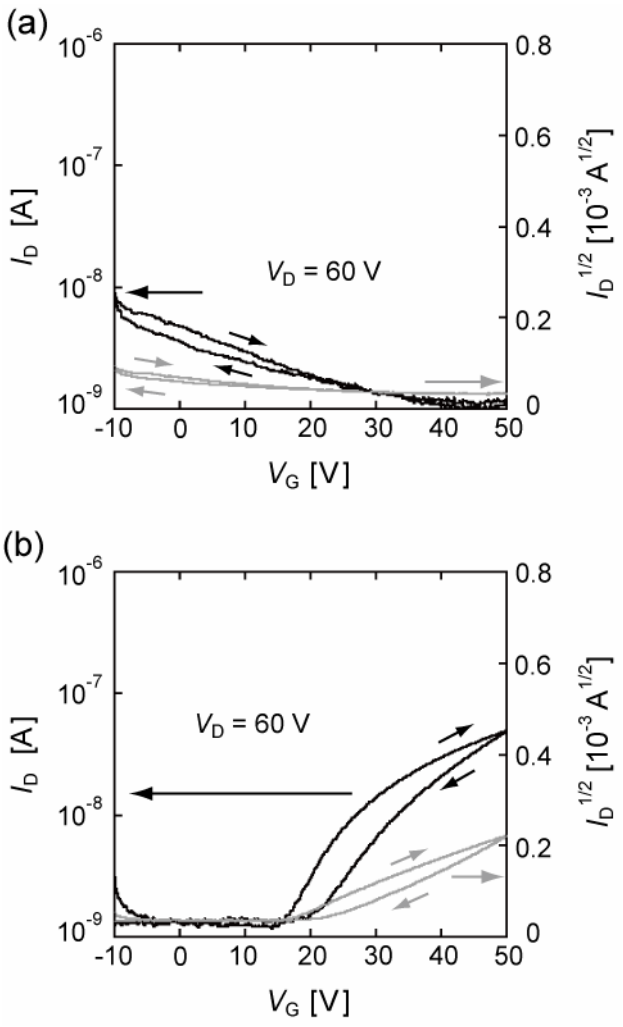

Fig. 5
S. Tanida et al.
(100%)